Vol 18 No 12, December 2009
1674-1056/2009/18(12)/5420-11

Chinese Physics B

© 2009 Chin. Phys. Soc.
and IOP Publishing Ltd

Multiple car-following model of traffic flow and numerical simulation*

Peng Guang-Han(彭光含)[a)b)†] and Sun Di-Hua(孙棣华)[a)]

[a)] *College of Automation, Chongqing University, Chongqing* 400044, *China*

[b)] *College of Physics and Electronics, Hunan University of Arts and Sciences, Changde* 415000, *China*

(Received 19 December 2008; revised manuscript received 1 June 2009)

On the basis of the full velocity difference (FVD) model, an improved multiple car-following (MCF) model is proposed by taking into account multiple information inputs from preceding vehicles. The linear stability condition of the model is obtained by using the linear stability theory. Through nonlinear analysis, a modified Korteweg-de Vries equation is constructed and solved. The traffic jam can thus be described by the kink–antikink soliton solution for the mKdV equation. The improvement of this new model over the previous ones lies in the fact that it not only theoretically retains many strong points of the previous ones, but also performs more realistically than others in the dynamical evolution of congestion. Furthermore, numerical simulation of traffic dynamics shows that the proposed model can avoid the disadvantage of negative velocity that occurs at small sensitivity coefficients λ in the FVD model by adjusting the information on the multiple leading vehicles. No collision occurs and no unrealistic deceleration appears in the improved model.

Keywords: traffic flow, optimal velocity model, numerical simulation
PACC: 6470, 0550, 0520

1. Introduction

Traffic flow is an interesting problem of modern society. To explain the complex properties of traffic, various traffic models have been developed, such as cellular automaton models, car-following models, hydrodynamic models and gas kinetic models.[1,2] The car-following model is one of the favorable microscopic traffic models that depict the motion of cars by differential equations. The optimal velocity (OV) model proposed by Bando *et al*[3] as one of the car-following models, has successfully described the formation of traffic jams and revealed the simplistic transition mechanism. The phase transitions between freely moving traffic and jammed traffic have been clarified by linear stability analysis. Subsequently, much work has been done based on the OV model.[4−34] Of this, some was induced by headways,[4−13] others considered the velocity difference.[14−30] Also, the interactions of both headways and velocity differences have been taken into account in a few models.[31−35]

In this paper, drivers may obtain multiple information on headways and velocity differences from leading vehicles by making use of the intelligent transportation system (ITS). Based on considering the effect of multiple information on leading vehicles, we propose a multiple car-following (MCF) model. Linear stability analysis shows that this new model is more stable than previous ones. Numerical simulation also shows that our model is more reasonable than others.

The paper is organized as follows. We review the performance of previous models on the evolution of congestion induced by a small perturbation in Section 2. In Section 3 we present the improved car-following model. In Section 4, linear stability analysis is conducted. In Section 5, nonlinear analysis is done. Acceleration and deceleration processes are carried out in Section 6. Both analytic and numerical methods of this model are used to analyse some observed physical features which exist in real traffic in Section 7. Finally we conclude the paper in Section 8.

2. Previous car-following models

2.1. The optimal velocity model

In 1995, Bando *et al*[3] proposed a simple microscopic traffic model called the optimal velocity model

*Project supported by the National High Tech Research and Development Program of China (Grant No 511-0910-1031) and the National "10th Five-year" Science and Technique Important Program of China (Grant No 2002BA404A07).

†Corresponding author. E-mail: pengguanghan@yahoo.com.cn

(for short, the OV model).[3] It was based on the idea that each vehicle has an optimal velocity, which depends on the following distance of the preceding vehicle. The motion of a vehicle n is described by the following equation

$$\frac{\mathrm{d}v_n(t)}{\mathrm{d}t} = a\left[V(\Delta x_n) - v_n(t)\right], \tag{1}$$

where $x_n(t)$ is the position of car n at time t, $\Delta x_n = x_{n+1} - x_n$ is the headway between car $n+1$ and car n at time t, a is the sensitivity of a driver, and V is the optimal velocity function (OVF). Helbing and Tilch carried out a calibration of the OV model with respect to the empirical data and suggested an OVF as[14]

$$V(\Delta x) = V_1 + V_2 \tanh\left[C_1(\Delta x - l_c) - C_2\right], \tag{2}$$

where $l_c = 5$ m is the length of the vehicles. The resulting optimal parameter values are $a = 0.85$ s^{-1}, $V_1 = 6.75$ m/s, $V_2 = 7.91$ m/s, $C_1 = 0.13$ m^{-1} and $C_2 = 1.57$. The comparison with field data suggests that high acceleration and unrealistic deceleration appear in the OV model.

2.2. The generalized force model

To overcome the shortage of the OV model, Helbing and Tilch[14] presented a generalized force (GF) model. Its formulation is as follows:

$$\frac{\mathrm{d}v_n(t)}{\mathrm{d}t} = a\left[V(\Delta x_n) - v_n(t)\right] + \lambda \Delta v_n H(-\Delta v_n), \tag{3}$$

where H is the Heaviside function, λ is a sensitivity coefficient different from a. $\Delta v_n(t)$ is the velocity difference between the preceding vehicle $n+1$ and the following vehicle n, $\Delta v_n(t) = v_{n+1} - v_n$. The calibration shows that in the GF model, $a = 0.41$ s^{-1}, which is much smaller than that in the OV model. The results also show that the GF model yields better agreement with the field data than the OV model.[14]

2.3. The full velocity difference model

In 2001, Jiang[15] *et al* pointed out that the GF model cannot describe the delay time δt and the kinematic wave speed at jam density c_j properly (see Table 1). By taking both positive and negative velocity differences into account, Jiang *et al* developed a full velocity difference model (for short, the FVD model).[15] The dynamic equation of a vehicle n is as follows:

$$\frac{\mathrm{d}v_n(t)}{\mathrm{d}t} = a\left[V(\Delta x_n) - v_n(t)\right] + \lambda \Delta v_n. \tag{4}$$

Numerical simulation shows that the FVD model gave a better description of the starting process than the GF model.[15]

Table 1. δt and c_j in different models.

model	a/s^{-1}	λ	m	δt/s	c_j/(km/h)
OV	0.85	0		1.6	16.65
GF	0.41	0.5		2.2	12.11
FVD	0.41	0.5	1	1.4	19.03
MCF	0.41	0.5	2	1.3	20.49
MCF	0.41	0.5	3	1.26	21.14

3. Model

Recently, by applying the ITS, drivers can receive information on other cars on the roads. Several traffic flow models have been proposed involving the use of ITS information[8−13,27−34] to enhance the stability of traffic flow. In order to improve the FVD model and considering the ITS application, we put forward a more useful model called the multiple car-following model (for short, the MCF model), which performs more realistically in the dynamical evolution of congestion, by taking into account the multiple information on preceding leading vehicles. Evidence shows that this new model is theoretically an improvement over the FVD model, while retaining many strong points of the previous ones. The dynamics equation reads

$$\begin{aligned}\frac{\mathrm{d}v_n(t)}{\mathrm{d}t} = {} & a\left[V(\Delta x_n, \Delta x_{n+1}, \ldots, \Delta x_{n+m-1}) - v_n(t)\right] \\ & + \lambda G(\Delta v_n, \Delta v_{n+1}, \ldots, \Delta v_{n+m-1}) \\ & (m \ll n),\end{aligned} \tag{5}$$

where m is the number of the front total vehicles considered in our model. $V(\bullet)$ represents optimal velocities considering m preceding vehicles. It is easy to know from Eq.(5) that the optimal velocities of the preceding vehicles are integrated into one synthesized optimal velocity function $V(\bullet)$, which is assumed in a linear form

$$\begin{aligned}& V(\Delta x_n, \Delta x_{n+1}, \ldots, \Delta x_{n+m-1}) \\ & = p_1 V(\Delta x_n) + p_2 V(\Delta x_{n+1}) + \cdots \\ & \quad + p_m V(\Delta x_{n+m-1}),\end{aligned} \tag{6}$$

where $G(\bullet)$ is a generic, monotonically increasing

function, and we assume a linear form as:

$$G(\Delta v_n, \Delta v_{n+1}, \ldots, \Delta v_{n+m-1}) = q_1\Delta v_n + q_2\Delta v_{n+1} + \cdots + q_m\Delta v_{n+m-1}. \tag{7}$$

In Eqs.(6) and (7)

$$\sum_{l=1}^{m} p_l = 1, \quad p_l = \begin{cases} \dfrac{p-1}{p^l} & \text{for} \quad l \neq m, \\ \dfrac{1}{p^{l-1}} & \text{for} \quad l = m, \end{cases}$$
$$\sum_{l=1}^{m} q_l = 1, \quad q_l = \begin{cases} \dfrac{q-1}{q^l} & \text{for} \quad l \neq m, \\ \dfrac{1}{q^{l-1}} & \text{for} \quad l = m, \end{cases} \tag{8}$$

where p_l and q_l are the weighting values, with $0 \leq p_l \leq 1$ and $0 \leq q_l \leq 1$, indicating the intensity with which the driver reacts to the preceding vehicle l. In our paper, $p = 2, 3, 4, \ldots$ and $q = 2, 3, 4, \ldots$ being a constant. It is well known that the influence of the vehicle ahead on vehicle motion reduces gradually as the distance between the considered vehicle and the vehicle ahead increases, which means $p_l > p_{l+1}$ and $q_l > q_{l+1}$. Also, an appropriate value of p_l and q_l could lead to desirable results. The model (5) conforms to the FVD model if $m = 1$, which only considers the effect of the nearest-neighbour ahead car.

4. Linear stability analysis

Linear stability analysis can be conducted for the MCF model as follows. It is obvious that the vehicles move with a uniform headway b and an optimal velocity $V(b, b, \ldots, b)$ is the steady state solution for Eq.(5), which is given by

$$x_n^0(t) = bn + V(b, b, \ldots, b)t \quad \text{with} \quad b = L/N, \tag{9}$$

where N is the total number of vehicles, and L is the road length. Suppose $y_n(t)$ is a small deviation from the steady-state solution $x_n^0(t) : x_n(t) = x_n^0(t) + y_n(t)$. Substituting it and Eqs.(6), (7) and (9) into Eq.(5) and linearizing the resultant equation yields

$$y''_n(t) = a\left[\sum_{l=1}^{m} p_l V'(b)\Delta y_{n+l-1} - y'_n(t)\right] + \lambda\left(\sum_{l=1}^{m} q_l \Delta y'_{n+l-1}\right), \tag{10}$$

where $\Delta y_n = y_{n+1}(t) - y_n(t)$, and $V'(b) = \mathrm{d}V(\Delta x_n)/\mathrm{d}\Delta x_n\,|_{\Delta x_n = b}$. By expanding $y_n(t)$, $y_n(t) = \mathrm{e}^{(\mathrm{i}\,\alpha_k n + zt)}$, in the Fourier models

$$z^2 + \left(a - \lambda\left(\sum_{l=1}^{m} q_l(\mathrm{e}^{\mathrm{i}\,kl} - \mathrm{e}^{\mathrm{i}\,k(l-1)})\right)\right)z - aV'(b)\left(\sum_{l=1}^{m} p_l(\mathrm{e}^{\mathrm{i}\,kl} - \mathrm{e}^{\mathrm{i}\,k(l-1)})\right) = 0, \tag{11}$$

where $z = z_1(\mathrm{i}\,k) + z_2(\mathrm{i}\,k)^2 + \cdots$, and inserting them into Eq.(5) gives the first- and second-order terms of coefficients in the expression of z respectively as follows:

$$z_1 = V'(b),$$
$$z_2 = \frac{a\sum\limits_{l=1}^{m} p_l(2l-1) + 2\lambda\sum\limits_{l=1}^{m} q_l}{2a}V'(b) - \frac{(V'(b))^2}{a}. \tag{12}$$

If z_2 is a negative value, the uniform steady-state flow becomes unstable for long-wavelength modes, while if z_2 is a positive value the uniform flow is stable. Thus the neutral stability condition is

$$V'(b) = \frac{a}{2}\sum_{l=1}^{m} p_l(2l-1) + \lambda. \tag{13}$$

For small disturbances with long wavelengths, the uniform traffic flow is stable if

$$V'(b) < \frac{a}{2}\sum_{l=1}^{m} p_l(2l-1) + \lambda. \tag{14}$$

When $m = 1$, the result of stable conditions is the same as that of the FVD model:[15]

$$V'(b) < \frac{a}{2} + \lambda. \tag{15}$$

Comparing the result with that of the FVD model, we can conclude that the improved model is stabilized in the region

$$\frac{a}{2} + \lambda < V'(b) < \frac{a}{2}\sum_{l=1}^{m} p_l(2l-1) + \lambda$$

by the effect of introducing multiple information on preceding vehicles, which means that the traffic flow becomes more stable than that in the FVD model by introducing multiple information on preceding vehicles into the original car-following model. It can also be found that the greater the number of preceding leading cars that are considered, the more stable the traffic will be.

The neutral stability line in the parameter space (b; a) for different m, as $m = 1$, 2, 3, 5, is shown in

Fig.1, where $\lambda = 0.5$ and $p = 3$. The neutral stability criterion presents the jamming transition curve among the free traffic, the inhomogeneous coexisting phase, and the homogeneous congested traffic. The apex of each curve indicates the critical point. The traffic flow is stable above the neutral stability line and a traffic jam will not appear, while below the line, traffic flow is unstable and density waves emerge. In addition, once the homogeneous traffic flow becomes unstable, the traffic flow evolves in time into an inhomogeneous jamming phase, which is characterized by the presence of an alternation pattern (congestion cluster) of high-density and low-density regions, and all vehicles in the platoon enter into a state of stop-and-go traffic after enough time. From Fig.1, it can be seen that the more vehicles ahead that are taken into account, the more the critical points and the neutral stability curves are lowered, which means that the more we consider the effects of information on preceding leading cars, the more stable the traffic will be. The traffic jam is thus suppressed efficiently. When $m = 1$, the neutral stability line is the same as that of the FVD model in a single-lane freeway.

Theoretically speaking, with the increase of m, the traffic flow becomes more stable. However, with the increase of m, information on more preceding leading vehicles needs be collected and processed too. According to Fig.1, when m=3, 5, the corresponding curves almost coincide, indicating that information on only three preceding leading vehicles (m=3) is enough to make the traffic become sufficiently stable under a small disturbance. Therefore, m=3 is the optimal state in the MCF model. That is to say, considering the effect of the three preceding leading vehicles on the following vehicle can suppress traffic jams effectively as well as save resources. Also, it implies that the model is more useful for the consideration of the effect of three preceding leading vehicles on the following car.

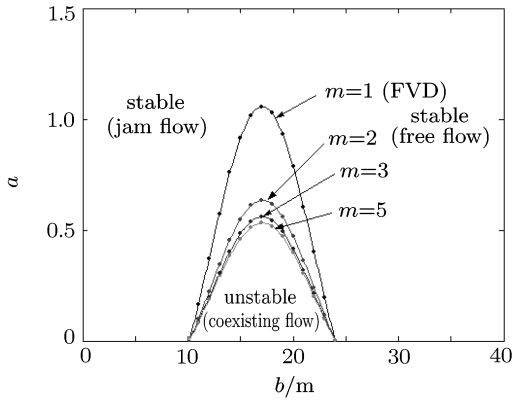


Fig.1. The neutral stability for different m.

5. Nonlinear analysis

For later convenience in nonlinear analysis, we rewrite Eq.(5) in the following form

$$\frac{\mathrm{d}^2(\Delta x(t))}{\mathrm{d}t^2} = a\left\{\left[\sum_{l=1}^{m} p_l V(\Delta x_{n+l}) - \sum_{l=1}^{m} p_l V(\Delta x_{n+l-1})\right]\frac{\mathrm{d}(\Delta x_n)}{dt}\right\} + \lambda\left[\sum_{l=1}^{m} q_l\left(\frac{\mathrm{d}(\Delta x_{n+l})}{\mathrm{d}t} - \frac{\mathrm{d}(\Delta x_{n+l-1})}{\mathrm{d}t}\right)\right]. \quad (16)$$

We choose the optimal velocity in a way similar to that proposed by Bando *et al*[3] for the convenience of nonlinear analysis:

$$V(\Delta x_n) = 0.5V_{\max}[\tanh(\Delta x_n - h_c) + \tanh(h_c)], \quad (17)$$

where h_c is the safety distance and $V_{\max}$ is the maximum velocity (for simplicity, $V_{\max}$ =2). When the headway is less than the safety distance, the vehicle reduces its velocity to prevent it from crashing into the preceding vehicle. On the other hand, if the headway is larger than the safety distance, it increases to the maximum velocity. We apply the reductive perturbation method to Eq.(16) and focus on the system behaviour near the critical point (h_c, a_c). With such a treatment, the nature of kink–antikink soliton solutions can be described by the mKdV equation. We introduce slow scales for the space variable n and the time variable t,[8,12] and define the slow variables X and T as:[8,12]

$$X = \varepsilon(n + bt), \quad (18)$$

$$T = \varepsilon^3 t, \quad (19)$$

where $\varepsilon = \sqrt{(a_c/a - 1)}$, $0 < \varepsilon \leq 1$, b is a constant to be determined. From the parabolic form of the neutral stability line near the critical point, it is expected that the amplitude of the density wave scales $c \propto \varepsilon$.[8,12] The headway is set to

$$\Delta x_n(t) = h_c + \varepsilon R(X, T). \tag{20}$$

Substituting Eqs.(18)–(20) into Eq.(16), and making the Taylor expansion to the fifth order of ε, we obtain the following nonlinear partial differential equation

$$\begin{aligned}
&\varepsilon^2[b - V']\partial_X R + \varepsilon^3\left[\frac{b^2}{a} - \frac{V'}{2}\sum_{l=1}^{m} p_l(2l-1) - \lambda\frac{b}{a}\right]\partial_X^2 R + \varepsilon^4\left\{\partial_T^2 R + \left[-\frac{V'}{6}\sum_{l=1}^{m} p_l(3l^2 - 3l + 1)\right.\right. \\
&\left.\left. - \lambda\sum_{l=1}^{m} q_l(2l-1)\frac{b}{2a}\right]\partial_X^3 R - \frac{V'''}{6}\partial_X R^3\right\} + \varepsilon^5\left\{\left(\frac{2b}{a} - \frac{\lambda}{a}\right)\partial_T\partial_X R + \left[-\frac{V'}{24}\sum_{l=1}^{m} p_l(4l^3 - 6l^2 + 4l - 1)\right.\right. \\
&\left.\left. - \frac{1}{24}\sum_{l=1}^{m} q_l(3l^2 - 3l + 1)\frac{\lambda b}{a}\right]\partial_X^4 R - \frac{V'''}{12}\sum_{l=1}^{m} p_l(2l-1)\partial_X^2 R^3\right\} = 0,
\end{aligned} \tag{21}$$

where $V' = \mathrm{d}V(\Delta x)/\mathrm{d}\Delta x|_{\Delta x = h_c}$, $V''' = \mathrm{d}^3 V(\Delta x)/\mathrm{d}\Delta x^3\big|_{\Delta x = h_c}$.

Near the critical point (a_c, h_c), with $b = V'$, $a_c/a = 1 + \varepsilon^2$ and eliminating the second- and third-order terms of ε from Eq.(21), equation (21) can be simplified to

$$\varepsilon^4[\partial_T R - g_1 V'\partial_X^3 R + g_2\partial_X R^3] + \varepsilon^5[\, g_3\partial_X^2 R + g_4\partial_X^4 R + g_5\partial_X^2 R^3] = 0, \tag{22}$$

where

$$g_1 = \frac{1}{6}V'\sum_{l=1}^{m} p_l(3l^2 - 3l + 1) + \frac{1}{2}\sum_{l=1}^{m} q_l(2l-1)\lambda V'/a_c, \tag{23a}$$

$$g_2 = -\frac{V'''}{6}, \quad g_3 = \frac{1}{2}V'\sum_{l=1}^{m} p_l(2l-1), \tag{23b}$$

$$\begin{aligned}
g_4 = &\left(\frac{2V'}{a_c} - \frac{\lambda}{a_c}\right)\left[\frac{V'}{6}\sum_{l=1}^{m} p_l(3l^2 - 3l + 1) + \frac{1}{2}\sum_{l=1}^{m} q_l(2l-1)\lambda V'/a_c\right] \\
&+ \left[-\frac{1}{24}V'\sum_{l=1}^{m} p_l(4l^3 - 6l^2 + 4l - 1) - \frac{1}{6}\sum_{l=1}^{m} q_l(3l^2 - 3l + 1)\lambda V'/a_c\right],
\end{aligned} \tag{23c}$$

$$g_5 = -\frac{1}{12}V'''\left[\sum_{l=1}^{m} p_l(2l-1) - 4V'/a_c - 2\lambda\right]. \tag{23d}$$

In order to obtain the standard mKdV equation, we use the transformations

$$T' = g_1 T, \quad R = \sqrt{\frac{g_1}{g_2}}R'. \tag{24}$$

Substituting Eq.(24) into Eq.(22), we obtain the regularized equation[8]

$$\partial_T R' - \partial_X^3 R' + \partial_X R'^3 + \varepsilon M[R'] = 0, \tag{25}$$

where

$$M[R'] = \sqrt{\frac{1}{g_1}}\left[g_3\,\partial_X^2 R' + \frac{g_1 g_5}{g_2}\partial_X^2 R'^3 + g_4\partial_X^4 R'\right]. \tag{26}$$

Equation (25) is the modified KdV equation with an $o(\varepsilon)$ correction term. First, we ignore the $o(\varepsilon)$ term in Eq.(25) and obtain the mKdV equation with the kink–antikink soliton solution

$$R'_0(X, T') = \sqrt{c}\tanh\sqrt{c/2}(X - cT'), \tag{27}$$

where c is the propagation velocity. In order to determine c for the solution of Eq.(25), the following requirement must be satisfied[8,12]

$$(R'_0, M[R'_0]) = \int_{-\infty}^{+\infty}\mathrm{d}X\, R'_0(X, T')M[R'_0(X, T')] = 0, \tag{28}$$

where $M[R'_0] = M[R']$. By solving the above equation, we obtain the selected velocity c for the kink–antikink solution according to the general solution pre-

sented by Ge *et al*[8]

$$c = 5g_2g_3/(2g_2g_4 - 3g_1g_5). \tag{29}$$

Hence, the kink–antikink soliton solution is of the form $(V' = 1,\ V''' = -2)$[8,12]

$$R(X,T) = \sqrt{\left[- V' \sum_{l=1}^{m} p_l(3l^2 - 3l + 1) + 3\sum_{l=1}^{m} q_l(2l-1)\lambda V'/a_{\rm c}\right] c/V'''} \times \tanh\sqrt{c/2}\left[X - cT\left(V'\sum_{l=1}^{m} p_l(3l^2-3l+1)/6\right) + \sum_{l=1}^{m} q_l(2l-1)\lambda V'/2a_{\rm c}\right]. \tag{30}$$

Thus the general kink–antikink soliton of the headway, i.e., the mKdV equation, is obtained

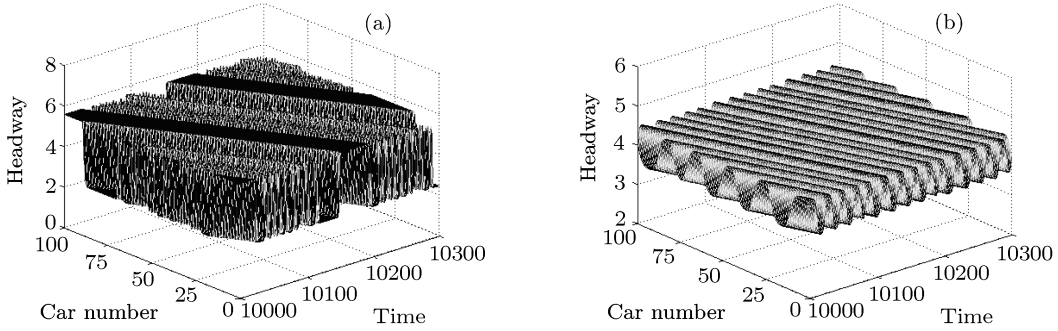
$$\Delta x_n(t) = h_{\rm c} + \sqrt{\left[- V' \sum_{l=1}^{m} p_l(3l^2 - 3l + 1) + 3\sum_{l=1}^{m} q_l(2l-1)\lambda V'/a_{\rm c}\right]\left(\frac{a_{\rm c}}{a} - 1\right) c/V'''} \times \tanh\sqrt{c/2}\left[X - cT\left(V'\sum_{l=1}^{m} p_l(3l^2-3l+1)/6\right) + \sum_{l=1}^{m} q_l(2l-1)\lambda V'/2a_{\rm c}\right]. \tag{31}$$

Here the amplitude A of the solution is

$$A = \sqrt{\left[- V' \sum_{l=1}^{m} p_l(3l^2 - 3l + 1) + 3\sum_{l=1}^{m} q_l(2l-1)\lambda V'/a_{\rm c}\right]\left(\frac{a_{\rm c}}{a} - 1\right) c/V'''}. \tag{32}$$

The kink–antikink solution represents coexisting phases, which consist of the freely moving phase at low density and the jammed (or congested) phase at high density. The headway of the freely moving phase and the jammed phase are given, respectively, by $\Delta x = h_{\rm c} + A$ and $\Delta x = h_{\rm c} - A$. When $m = 1$, the result is similar to that solved by Xue *et al.*[16]

To validate the results of the theoretical analysis, numerical simulation has been carried out for the MCF model described by Eq.(5), in which the periodical boundary conditions are used. The initial conditions are given as follows: $\Delta x_j(0) = \Delta x_0 = 4$, $\Delta x_j(1) = \Delta x_0 = 4.0$ for $j \neq 50,\ 51$, $\Delta x_j(1) = 4.0 - 0.5$ for $j = 50$, and $\Delta x_j(1) = 4.0 + 0.5$ for $j = 51$, where the total number of cars is $N = 100$. The safety distance is $h_{\rm c} = 4$, and other input parameters are $a = 1.5$, $\lambda = 0.1$, $V_{\max} = 2$, $p = 3$, $q = 2$. Figure 2 shows the space-time evolution of the headways for different cars considered. In Fig.2, the traffic jams abate gradually for Figs.2(a)–2(d) with increasing value of m. It thus can be concluded that the traffic jam can be suppressed more effectively by taking into account ITS information of multiple preceding leading vehicles than by considering only one preceding car. In Fig.2, the kink–antikink soliton solution appears as a traffic jam and the density waves propagate backwards. The simulation results are in good agreement with the analytical ones.



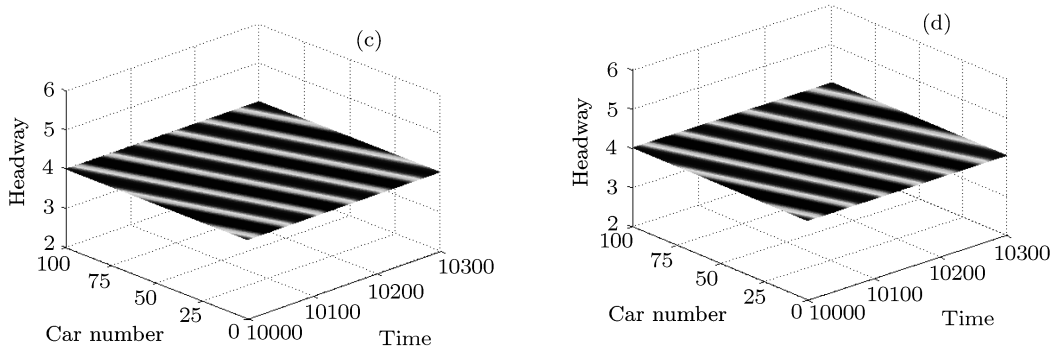


Fig.2. Space-time evolution of the headways after $t = 10000$. The patterns (a)–(d) are for the coexisting phases corresponding to the cases of $m = 1$, 2, 3 and 5 respectively.

Figure 3 shows the headway profile obtained at a sufficiently long time, $t = 10300$. With the same sensitivity, as the number of preceding leading cars increases, the amplitude of the density wave decreases. In patterns (c) and (d) the density waves disappear and traffic flow is uniform over the whole space. Therefore, the simulation outcomes are in agreement with the analytical results.

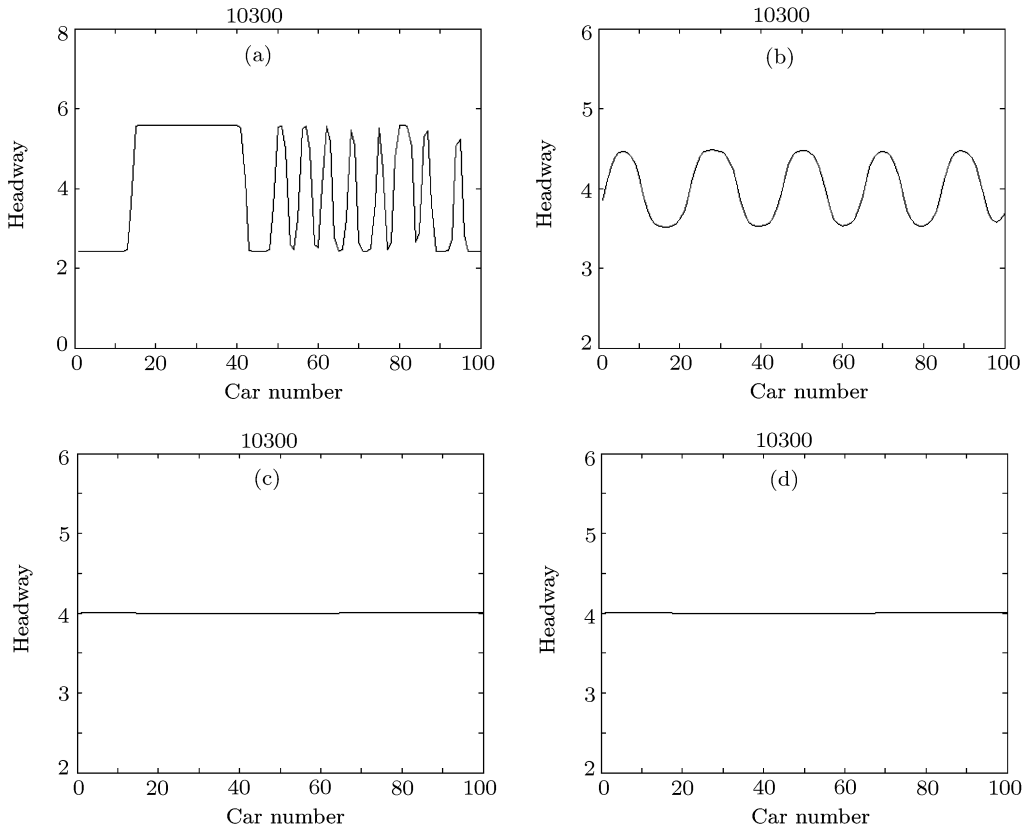


Fig.3. Headway profile of the density waves at $t = 10300$. The patterns (a), (b), (c), and (d) correspond to $m = 1$, 2, 3, and 5, respectively.

6. Starting and braking processes

Firstly, we apply the MCF model to simulate car motion under a traffic signal and examine certain properties of the MCF model. We carry out the same simulation as that in Ref.[15]. First, the traffic signal is red and all vehicles are waiting with a headway of 7.4 m, where the optimal velocity is zero. Then at time $t = 0$, the signal changes to green and the ve-

hicles start. We define the delay time of car motion by δt as that in the FVD model, which is related to the different values of m. Then, we can estimate the kinematic wave speed at jam density $c_j = 7.4/\delta t$. For comparison, we use the same parameters as those in the FVD model. The simulation results are shown in Fig.4 and Table 1. From Table 1, we can see that the observed δt is of the order of 1 s, just as Bando *et al*[36] pointed out, and c_j ranges between [17 km/h, 23 km/h].[37] Therefore, the MCF model is successful in anticipating the two parameters. With increasing m, delay time δt and kinematic wave speed c_j approach more exactly the observed values.

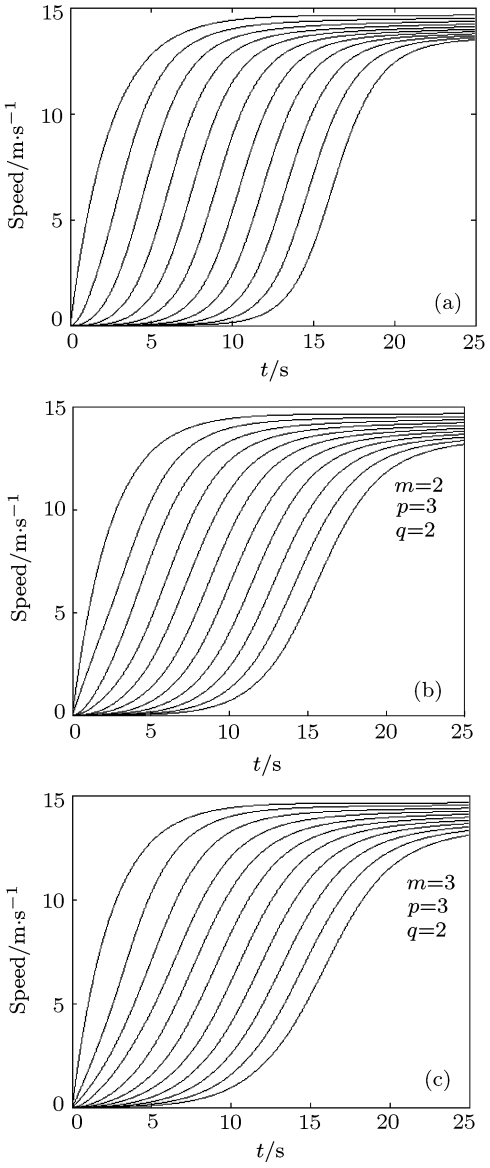


Fig.4. Motions of vehicles 1–11 starting from a traffic signal: (a) FVD ($m = 1$); (b) MCF ($m = 2$); (c) MCF ($m = 3$).

Also, the variations of all vehicles' acceleration are shown in Fig.5 according to the FVD model and the MCF model respectively, where the solid line represents the leading car, and the dashed lines represent the following vehicles. Since empirical deceleration and acceleration are limited between the range [–3 m/s^2, 4 m/s^2],[14] from Fig.5 we can see that the maximum value of acceleration in the MCF model is not greater than that in the FVD model, which is not beyond the limitation of 4 m/s^2.

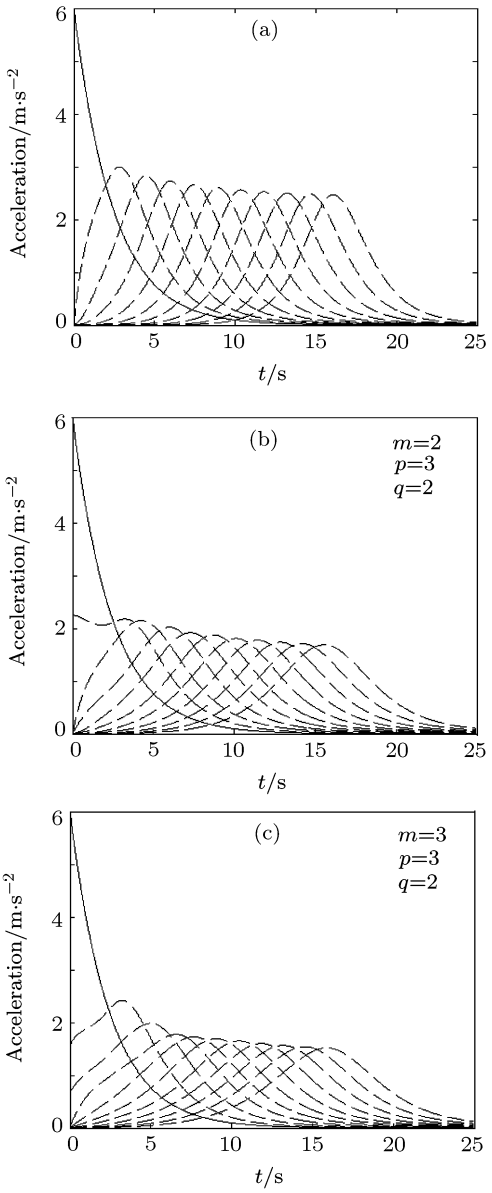


Fig.5. Acceleration of leading vehicle and its following vehicles: (a) FVD ($m = 1$); (b) MCF ($m = 2$); (c) MCF ($m = 3$).

Finally, we simulate the deceleration process of the vehicles, which was not simulated in Ref.[15]. In Fig.6, the solid line represents the leading vehicle, and the broken lines represent the following vehicles. According to Fig.6, the FVD model has too high a deceleration, while the MCF model does not show unre-

alistically high deceleration.

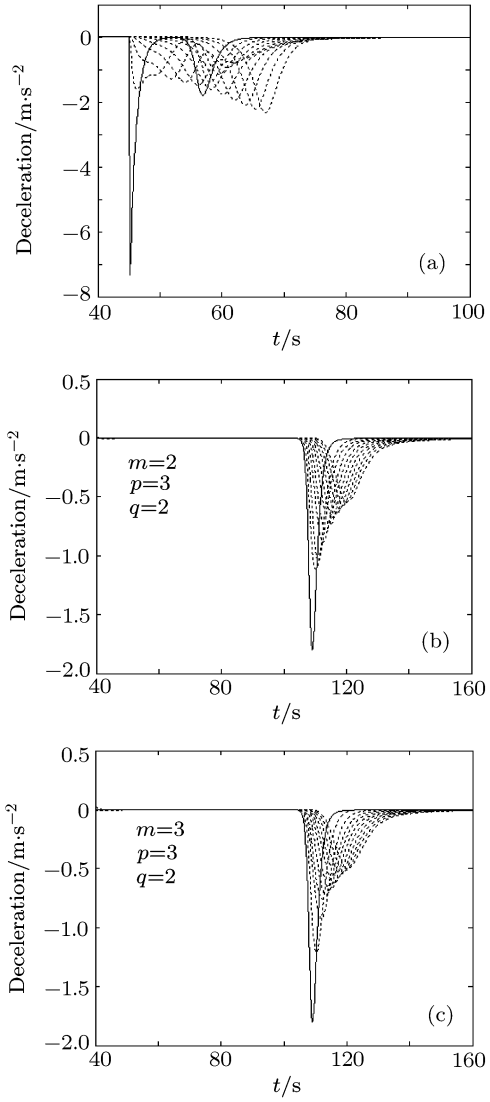


Fig.6. Deceleration of leading vehicle and its following vehicles: (a) FVD ($m = 1$); (b) MCF ($m = 2$); (c) MCF ($m = 3$).

7. Numerical simulation

A numerical simulation is carried out to observe the traffic dynamics in the MCF model. For comparison, we take Eq.(2) for the optimal velocity function and the same parameters as in the FVD model. There are $N = 100$ vehicles running on a road with a length of $L = 1500$ m, under a periodic boundary condition. We set the same initial disturbance as that in Ref.[15]

$$x_1(0) = 1 \text{ m}, \ \ x_n(0) = [(n-1)L/N] \text{ m}, \text{ for } n \neq 1; \quad (33)$$

$$\dot{x}_n(0) = V(L/N). \quad (34)$$

Other parameters are: $a = 0.41$, $b = L/N$, $p = 3$, $q = 2$.

First we consider the case of the FVD model at different values of λ. In order to gain an insight into the information on the variation of vehicles, snapshots of the velocities of all vehicles at $t = 300$ s and $t = 1000$ s for the FVD model are shown in Figs.7 and 8 respectively. We see clearly from the figure that vehicle velocities tend to come to the two typical values as time develops. The homogeneous flow eventually develops into congestion, which corresponds to stop-and-go traffic. However, we clearly observe the appearance of negative velocity in the low-density region in the case of $\lambda = 0.3$ and $\lambda = 0.4$ in the FVD model, which is very unrealistic and not allowed in real traffic. By taking into account the information on the two leading vehicles ($m = 2$), the MCF model can avoid the disadvantage of negative velocity occurring in the case of $\lambda = 0.4$ in the FVD model from Fig.9. But there still exists the appearance of negative velocity in the case of $\lambda = 0.3$ in Fig.9, indicating that it is necessary and important to consider more than two leading vehicles for the following car. Therefore, our model also

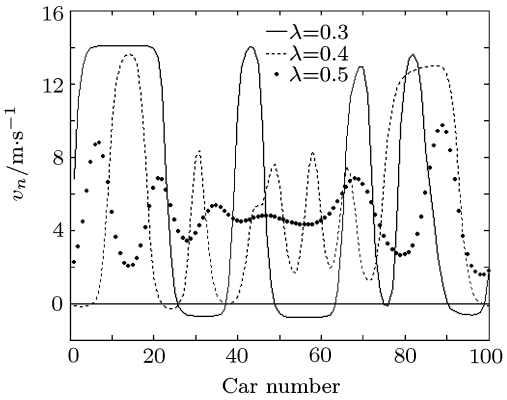


Fig.7. Snapshot of the velocities of all vehicles at different values of λ when $t = 300$ s in the FVD model.

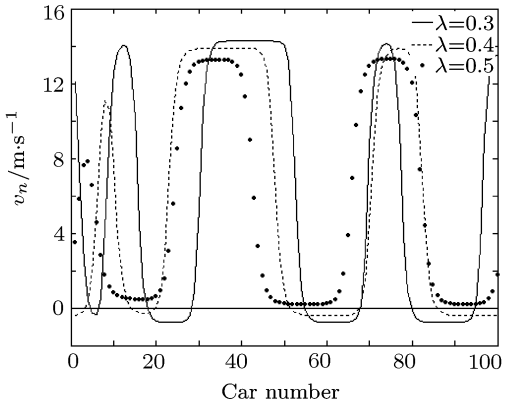


Fig.8. Snapshot of the velocities of all vehicles at different values of λ when $t = 1000$ s in the FVD model.

dominates over others in the case when only two leading vehicles are taken into account. By taking into account the information on the three leading vehicles ($m = 3$), the MCF model can avoid the disadvantage of negative velocity that occurs in the case of $\lambda = 0.3$ or $\lambda = 0.4$ in the FVD model from Fig.10. Also, the amplitude of the curves decreases with increasing m from 1–3 for all values of λ. In other words, the more vehicles that are taken into account, the more stable the uniform traffic flow is.

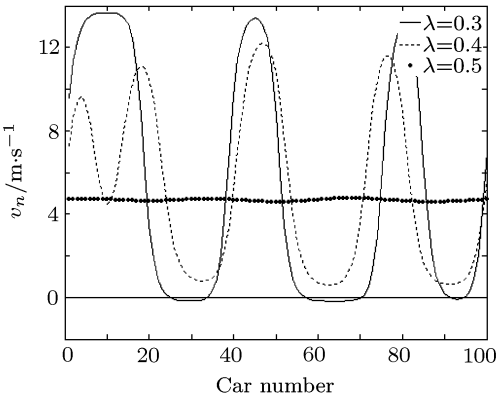


Fig.9. Snapshot of the velocities of all vehicles at different values of λ when $t = 1000$ s in the MCF model ($m = 2$).

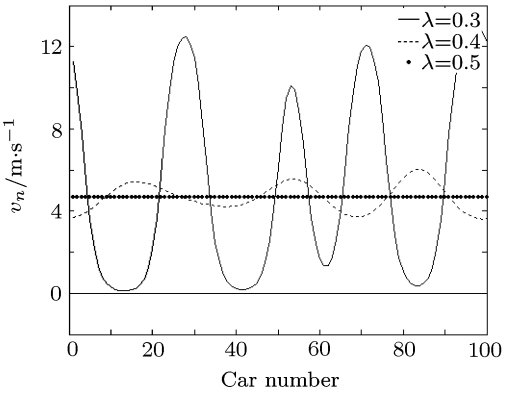


Fig.10. Snapshot of the velocities of all vehicles at different values of λ when $t = 1000$ s in the MCF model ($m = 3$).

The realistic value of λ in real traffic was found to lie between 0.3 and 0.7.[23] The velocity-headway trajectory in the MCF model is compared with that in the FVD model as follows. A closed trajectory called a hysteresis loop is clearly observed in the FVD and MCF models. When the traffic flow becomes stationary after a sufficiently long time, the motion of all vehicles forms a loop as shown in Figs.11, 12 and 13. Changing the value of λ, loops of different sizes can be obtained in the FVD model (see Fig.11), which is the same as that in Ref.[15]. From Fig.11 we see that the unrealistic phenomena of negative velocity will appear if the condition of $\lambda < 0.5$ is satisfied in the FVD model (for example, points F and G). When $\lambda = 0.8$,

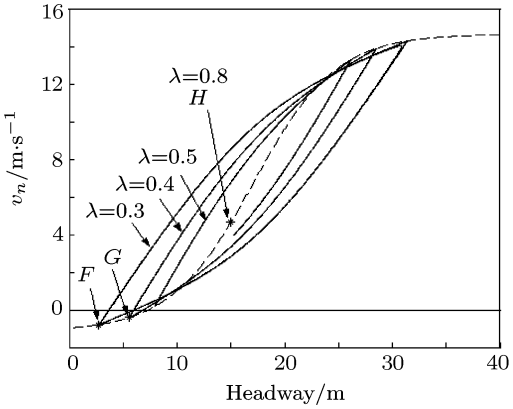


Fig.11. Loops for the FVD model at different values of λ. The dashed curve represents OVF.

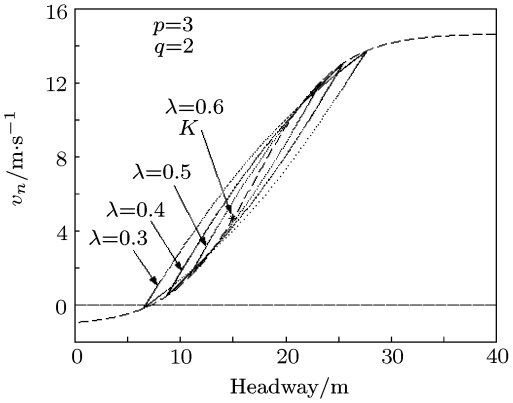


Fig.12. Loops for the MCF model at different values of λ when $m = 2$. The dashed curve represents OVF.

criterion (15) holds, the traffic flow is stable, the hysteresis loop will not be generated, and in phase space, there will be only a point H on the optimal velocity curve instead. From Fig.12, by considering the information on two leading vehicles, the unrealistic negative velocity never appears at $\lambda = 0.4$ in the MCF model. However, when $\lambda = 0.3$, unrealistic negative velocity still occurs even though it improves the traffic at $m = 2$, which is in accordance with the result in Fig.9. When $m = 3$, loops of different sizes were formed and the desired values of λ never fall into a negative velocity regime in Fig.13. From this point of view, the MCF model describes the traffic dynamics more exactly when the value of m is over 2, which further verifies that the modified FVD model is more reasonable and realistic than previous ones. When $\lambda = 0.6$, criterion (14) holds, the traffic flow is stable, the hysteresis loop will not be generated, and in

phase space, there will be only a point (K, L) on the optimal velocity curve instead. Obviously, λ decreases with increasing m under stable traffic flow.

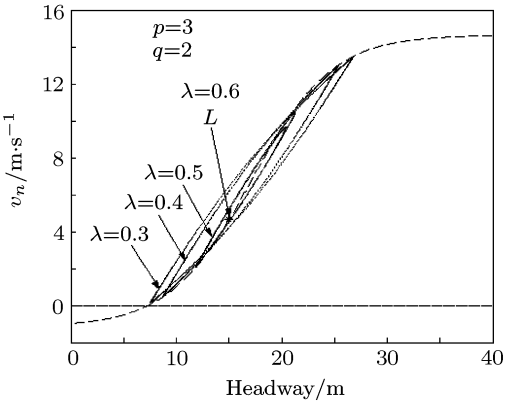


Fig.13. Loops for the MCF model at different values of λ when $m = 3$. The dashed curve represents OVF.

8. Conclusions

This paper introduces an improved MCF model for a single lane car-following theory, performing more realistically in both acceleration and deceleration processes than the FVD model by taking multiple leading vehicles into account. The key improvement in the FVD model is that the MCF model can exactly avoid the disadvantage of negative velocity that occurs at small sensitivity coefficients λ in the FVD model, where no unrealistic deceleration appears and no collision occurs. Linear stability analysis has been done and the stable criterion is given. The kink–antikink soliton solution of the mKdV equation near the critical point is derived to describe the traffic jams. From the numerical simulation, we can conclude that traffic jams are suppressed efficiently by taking into account information on more leading cars. Also, the simulation results directly indicate that the preceding vehicle term has an important impact on traffic dynamics.

References

[1] Chowdhury D, Santen L and Schadschneider A 2000 *Phys. Rep.* **329** 199
[2] Helbing D 2001 *Rev. Mod. Phys.* **73** 1067
[3] Bando M, Hasebe K, Nakyaama A, Shibata A and Sugiyama Y 1995 *Phys. Rev.* E **51** 1035
[4] Li X L, Song T, Kuang H and Dai S Q 2008 *Chin. Phys.* B **17** 3014
[5] Hayakawa H and Nakanishi K 1998 *Prog. Theor. Phys. Suppl.* **130** 57
[6] Nagatani T 1999 *Phys. Rev.* E **60** 6395
[7] Lenz H and Wagner C K 1999 *Eur. Phys. J.* B **7** 331
[8] Ge H X, Dai S Q, Dong L Y and Xue Y 2004 *Phys. Rev.* E **70** 066134
[9] Wagner C K 1998 *Physica* A **260** 218
[10] Hasebe K, Nakayama A and Sugiyama Y 2003 *Phys. Rev.* E **68** 026102
[11] Sawada S 2002 *Int. J. Mod. Phys.* C **13** 1
[12] Ge H X, Dai S Q, Xue Y and Dong L Y 2005 *Phys. Rev.* E **71** 066119
[13] Zhu H B and Dai S Q 2008 *Physica* A **387** 3290
[14] Helbing D and Tilch B 1998 *Phys. Rev.* E **58** 133
[15] Jiang R, Wu Q S and Zhu Z J 2001 *Phys. Rev.* E **64** 017101
[16] Xue Y 2003 *Acta Phys. Sin.* **52** 2750 (in Chinese)
[17] Xue Y, Dong L Y, Yuan Y W and Dai S Q 2002 *Acta Phys. Sin.* **51** 492 (in Chinese)
[18] Xue Y 2002 *Chin. Phys.* **11** 1128
[19] Tang T Q, Huang H J and Gao Z Y 2005 *Phys. Rev.* E **72** 066124
[20] Wang T, Gao Z Y and Zhao X M 2006 *Acta Phys. Sin.* **55** 634 (in Chinese)
[21] Li L and Shi P F 2005 *Chin. Phys.* **14** 0576
[22] Zhao X M and Gao Z Y 2005 *Eur. Phys. J.* B **47** 145
[23] Li Z P and Liu Y C 2006 *Chin. Phys.* **15** 1570
[24] Sawada S 2006 *Int. J. Mod. Phys.* C **17** 65
[25] Li Z P, Liu Y C and Liu F Q 2007 *Int. J. Mod. Phys.* C **18** 819
[26] Li Z P, Gong X B and Liu Y C 2006 *Commun. Theor. Phys.* **46** 367
[27] Ge H X, Zhu H B and Dai S Q 2006 *Eur. Phys. J.* B **54** 503
[28] Lei Y and Shi Z K 2008 *Chaos, Solitons and Fractals* **36** 550
[29] Gong H X, Liu H C and Wang B H 2008 *Physica* A **387** 2595
[30] Ge H X 2008 *Physica* A **360** 1
[31] Zhu W X and Liu Y C 2008 *J. Shanghai Jiaotong Univ. (Sci. ed.)* **13** 166
[32] Xie D F, Gao Z Y and Zhao X M 2008 *Commun. Comput. Phys.* **3** 899
[33] Peng G H, Sun D H and He H P 2008 *Acta Phys. Sin.* **57** 7541 (in Chinese)
[34] Mo Y L, He H D, Xue Y, Shi W and Lu W Z 2008 *Chin. Phys.* B **17** 4446
[35] Tang T Q, Huang H J, Wong S C and Jiang R 2009 *Chin. Phys.* B **18** 975
[36] Bando M, Hasebe K, Nakanishi K and Nakayama A 1998 *Phys. Rev.* E **58** 5429
[37] Del Castillo J M and Benitez F G 1995 *Transp. Res.* B **29** 373